

SCIENTIFIC REPORTS



OPEN

Effect of caloric restriction on gut permeability, inflammation markers, and fecal microbiota in obese women

Beate Ott^{1,2}, Thomas Skurk^{1,2}, Ljiljana Hastreiter¹, Ilias Lagkouravdos^{1,2}, Sandra Fischer², Janine Büttner³, Teresa Kellerer¹, Thomas Clavel^{2,4}, Michael Rychlik⁵, Dirk Haller^{2,6} & Hans Hauner^{1,2,7}

Recent findings suggest an association between obesity, loss of gut barrier function and changes in microbiota profiles. Our primary objective was to examine the effect of caloric restriction and subsequent weight reduction on gut permeability in obese women. The impact on inflammatory markers and fecal microbiota was also investigated. The 4-week very-low calorie diet (VLCD, 800 kcal/day) induced a mean weight loss of 6.9 ± 1.9 kg accompanied by a reduction in HOMA-IR (Homeostasis model assessment-insulin resistance), fasting plasma glucose and insulin, plasma leptin, and leptin gene expression in subcutaneous adipose tissue. Plasma high-molecular weight adiponectin (HMW adiponectin) was significantly increased after VLCD. Plasma levels of high-sensitivity C-reactive protein (hsCRP) and lipopolysaccharide-binding protein (LBP) were significantly decreased after 28 days of VLCD. Using three different methods, gut paracellular permeability was decreased after VLCD. These changes in clinical parameters were not associated with major consistent changes in dominant bacterial communities in feces. In summary, a 4-week caloric restriction resulted in significant weight loss, improved gut barrier integrity and reduced systemic inflammation in obese women.

A chronic positive energy balance leads to obesity and low-grade inflammation. This subclinical inflammatory state is considered to pave the way for insulin resistance and subsequent type 2 diabetes mellitus^{1,2} and to promote cardiovascular diseases³. However, the reasons for this low-grade inflammation are poorly understood. It may, in part, be explained by macrophage infiltration into adipose tissue^{4,5}. Furthermore, adipocyte hypertrophy and the associated dysregulated adipokine secretion profile may contribute to inflammation⁶. Recent studies suggested that increased gut permeability⁷ and lipopolysaccharides (LPS) translocation may also play an important role^{8,9}. Some evidence exists that BMI is a major covariate of microbiome variations and that obesity is associated with changes in intestinal microbiota composition^{10–13}. A disrupted gut barrier function may lead to an increased influx of bacterial components such as LPS^{9,14,15} and other complex antigens into the circulation and, thereby, activate immune responses^{8,16}. It is currently speculated that increased gut permeability can be caused by microbial imbalance, food composition (e.g. gluten)^{17,18} or high-calorie diets^{19,20}. In contrast, weight reduction is known to improve metabolic disturbances and to decrease the systemic inflammatory tone^{21,22}.

Based on the observation that obesity is associated with a chronic low-grade inflammatory state and, potentially, impaired gut permeability⁷, the present study aimed to investigate whether caloric restriction is able to modulate gut permeability and, thereby, decrease markers of inflammation in human subjects. Moreover, gut

¹Else Kröner-Fresenius-Center of Nutritional Medicine, Technical University of Munich, Freising, Germany. ²ZIEL Institute for Food and Health, Technical University of Munich, Freising-Weihenstephan, Germany. ³Charité-Universitätsmedizin, Medizinische Klinik mit Schwerpunkt Hepatologie und Gastroenterologie, Berlin, Germany. ⁴Institute of Medical Microbiology, RWTH University Hospital, Aachen, Germany. ⁵Chair of Analytical Food Chemistry, Technical University of Munich, Freising, Germany. ⁶Chair of Nutrition and Immunology, Technical University of Munich, Freising-Weihenstephan, Germany. ⁷Institute of Nutritional Medicine, Klinikum rechts der Isar, Technical University of Munich, Munich, Germany. Correspondence and requests for materials should be addressed to H.H. (email: hans.hauner@tum.de)

| | before VLCD (n = 20) | after VLCD (n = 20) | 14d after VLCD (n = 20) | p - value |
|------------------------------|----------------------|---------------------|-------------------------|-----------|
| | t1 | t2 | t3 | t1–t2 |
| Weight (kg) | 95.1 ± 13.4 | 88.2 ± 12.3 | 88.5 ± 12.6 | <0.001 |
| BMI (kg/m ²) | 34.9 ± 3.8 | 32.5 ± 3.5 | 32.6 ± 3.8 | <0.001 |
| Waist circumference (cm) | 106.9 ± 10.6 | 101.2 ± 9.4 | 100.5 ± 9.3 | <0.001 |
| Hip circumference (cm) | 118.5 ± 12.6 | 113.9 ± 10.8 | 114.4 ± 11.5 | <0.001 |
| Lean mass (kg) | 52.7 ± 5.7 | 50.0 ± 5.5 | 50.9 ± 5.3 | <0.001 |
| Fat mass (kg) | 42.5 ± 8.8 | 38.2 ± 7.9 | 37.6 ± 8.4 | <0.001 |
| RMR (kJ/day) | 7,016 ± 109 | 6,689 ± 707 | 7,061 ± 716 | 0.07 |
| Total cholesterol (mmol/L) | 4.9 ± 1.0 | 4.2 ± 0.8 | 4.8 ± 0.9 | <0.001 |
| HDL-c (mmol/L) | 1.3 ± 0.2 | 1.1 ± 0.2 | 1.3 ± 0.3 | <0.001 |
| LDL-c (mmol/L) | 3.1 ± 0.9 | 2.6 ± 0.7 | 2.9 ± 0.8 | <0.001 |
| Triglycerides (mmol/L) | 1.4 ± 0.7 | 1.1 ± 0.5 | 1.3 ± 0.7 | 0.05 |
| LDL/HDL | 2.4 ± 0.8 | 2.3 ± 0.7 | 2.2 ± 0.7 | 0.68 |
| NEFA (mmol/L) | 0.6 ± 0.2 | 0.7 ± 0.2 | 0.5 ± 0.2 | 0.03 |
| Fasting glucose (mmol/L) | 4.8 ± 0.7 | 4.5 ± 0.6 | 4.7 ± 0.6 | <0.001 |
| Glucose 120 minutes (mmol/L) | 6.5 ± 2.4 | 6.8 ± 1.3 | not assessed | 0.16 |
| Fasting insulin (pmol/L) | 63.7 ± 44.6 | 44.3 ± 20.6 | 59.7 ± 62.9 | <0.001 |
| HOMA-IR | 2.05 ± 1.52 | 1.29 ± 0.68 | 1.77 ± 1.82 | <0.001 |
| hsCRP (µg/L) | 3.1 ± 3.7 | 1.7 ± 1.6 | 2.7 ± 2.6 | <0.01 |
| HMW Adiponectin (µg/L) | 4.1 ± 2.2 | 4.7 ± 2.7 | 4.9 ± 2.8 | <0.01 |
| Leptin (µg/L) | 43.8 ± 25.2 | 20.9 ± 16.1 | 25.9 ± 20.3 | <0.001 |
| RANTES (µg/L) | 47.6 ± 19.3 | 45.6 ± 22.6 | 39.8 ± 24.1 | 0.28 |
| MCP-1 (ng/L) | 82.1 ± 32.6 | 84.5 ± 23.4 | 89.1 ± 25.5 | 0.5 |
| Chemerin (µg/L) | 77.6 ± 25.7 | 64.8 ± 20.2 | 75.7 ± 21.1 | <0.01 |
| LBP (µg/L) | 27.3 ± 3.3 | 25.8 ± 3.5 | 28.0 ± 3.5 | <0.01 |
| Calprotectin (µg/L) | 424.9 ± 560.3 | 342.9 ± 351.6 | 142.9 ± 132.9 | 0.85 |

Table 1. Anthropometric and metabolic characteristics of study participants. Data are presented as mean ± standard deviation. P-value for differences between time points before and after VLCD was determined using paired Student's test.

microbiota diversity and composition, and their possible association with gut permeability and inflammation was investigated.

Results

The calorie-restricted formula diet induced weight loss. Twenty women (mean age 46.8 ± 11.5) were included in the study and no participant dropped out. Physical and biochemical characteristics of the participants before intervention, immediately after the hypocaloric diet, and 14d after intervention are shown in Table 1. Participants were asked to consume a formula diet (800 kcal/day) and, in addition, 200 g vegetables. Compared to the original caloric intake of 1,698.1 ± 592.7 kcal/day, this intervention caused a substantial energy deficit ($P < 0.0001$).

The VLCD resulted in a significant decrease in body weight (-6.9 ± 1.9 kg). This corresponded to a decrease in BMI (-2.5 ± 0.7 kg/m²), lean mass (-2.7 ± 1.6 kg), and total body fat mass (-4.2 ± 1.6 kg). In addition, waist circumference (-5.7 ± 5.5 cm) and hip circumference (-4.5 ± 3.7 cm) were significantly decreased. RMR did not change significantly during the 4 weeks of dietary intervention (Table 1).

During the two weeks following the intervention, participants regained on average 250 ± 1.5 g body weight ($P = 0.47$). Waist circumference ($P = 0.44$) and hip circumference ($P = 0.64$) did not change significantly during this post-study period. However, lean mass ($P = 0.01$) significantly increased and fat mass ($P = 0.02$) significantly decreased during the last two weeks.

Caloric restriction improved metabolic and inflammatory markers transiently. Total cholesterol, high-density lipoprotein cholesterol (HDL-c), low-density lipoprotein cholesterol (LDL-c), and triglycerides decreased significantly following VLCD (Table 1). During the subsequent two weeks, these parameters increased again ($P < 0.001$ each). In addition, we observed a significant ($P = 0.03$) increase in nonesterified fatty acids (NEFA) during VLCD. During the subsequent two weeks, NEFA decreased significantly ($P < 0.0001$). Regarding glucose metabolism, fasting glucose (from 4.8 ± 0.7 mmol/L to 4.5 ± 0.6 mmol/L), plasma insulin (from 63.7 ± 44.6 pmol/L to 44.3 ± 20.6 pmol/L), and HOMA-IR index (from 2.05 ± 1.52 to 1.29 ± 0.68) were significantly lower ($P < 0.001$ each) after VLCD compared to baseline. During the last two weeks of the study (after returning to the habitual diet), blood glucose significantly increased ($P = 0.04$), whereas insulin levels ($P = 0.11$) and HOMA-IR did not change significantly ($P = 0.16$). Post-glucose concentrations during the glucose tolerance test did not change significantly before and after VLCD ($P = 0.16$, Table 1).

| | n | before VLCD | after VLCD | 14d after VLCD | p - value |
|---|----|--------------|---------------|----------------|-----------|
| | | t1 | t2 | t3 | t1 - t2 |
| Sucrose (urine recovery in %) | 18 | 0.17 ± 0.12 | 0.10 ± 0.06 | 0.73 ± 0.94 | 0.01 |
| Mannitol (urine recovery in %) | 18 | 12.35 ± 5.38 | 9.30 ± 4.99 | 14.66 ± 9.16 | 0.17 |
| Lactulose (urine recovery in %) | 18 | 0.26 ± 0.18 | 0.15 ± 0.10 | 0.32 ± 0.32 | 0.01 |
| Sucralose, urine recovery in % | 18 | 1.09 ± 1.52 | 0.26 ± 0.48 | 1.30 ± 1.79 | 0.02 |
| PEG ₉ (urine recovery in %) | 20 | 16.8 ± 10.34 | 12.4 ± 7.29 | 16.6 ± 12.7 | 0.03 |
| PEG ₁₁ (urine recovery in %) | 20 | 16.5 ± 15.15 | 7.6 ± 5.57 | 17.3 ± 19.5 | 0.01 |
| PEG ₁₃ (urine recovery in %) | 20 | 4.2 ± 3.59 | 2.14 ± 1.25 | 4.2 ± 4.1 | <0.01 |
| PEG ₂₅ (urine recovery in %) | 20 | 0.38 ± 0.33 | 0.17 ± 0.15 | 0.30 ± 0.28 | <0.001 |
| PEG ₃₀ (urine recovery in %) | 20 | 0.22 ± 0.17 | 0.11 ± 0.08 | 0.15 ± 0.12 | <0.001 |
| PEG ₃₅ (urine recovery in %) | 20 | 0.20 ± 0.18 | 0.08 ± 0.09 | 0.15 ± 0.20 | <0.001 |
| PEG ₄₀ (urine recovery in %) | 20 | 0.24 ± 0.24 | 0.10 ± 0.11 | 0.16 ± 0.19 | <0.01 |
| PEG ₇₀ (urine recovery in %) | 20 | 0.1 ± 0.08 | 0.04 ± 0.08 | 0.04 ± 0.06 | 0.02 |
| PEG ₈₀ (urine recovery in %) | 16 | 0.04 ± 0.05 | 0.02 ± 0.04 | 0.02 ± 0.04 | 0.09 |
| Plasma Zonulin (µg/L) | 20 | 58.4 ± 21.7 | 47.45 ± 11.88 | 54.34 ± 14.75 | <0.01 |

Table 2. Gut permeability parameters at three different time point. Data are presented as means ± standard deviation. P-value for differences between time points before and after VLCD was determined using paired Student's test.

The hypocaloric diet induced a decrease in the inflammation marker hsCRP (Table 1). HMW adiponectin increased and leptin decreased ($P < 0.001$ each) after VLCD. The chemokines regulated on activation normal T cell expressed and secreted (RANTES) and monocyte chemoattractant protein-1 (MCP-1) did not change significantly during the whole study. Chemerin, considered to be a marker of inflammation and to be associated with obesity and the metabolic syndrome^{23,24}, showed a significant decrease after caloric restriction ($P < 0.01$). LBP levels, a marker for translocation of cell-wall components from Gram-negative bacteria, significantly decreased after intervention ($P < 0.01$) and increased again during follow-up ($P < 0.0001$). Fecal calprotectin did not decrease significantly after VLCD ($P = 0.79$).

Markers of paracellular gut permeability decreased during VLCD. Table 2 summarises the results obtained using different approaches for measurement of gut permeability. In brief, paracellular gut permeability markers, including lactulose, polyethylene glycol (PEG) 1500 (PEG₂₅, PEG₃₀, PEG₃₅, and PEG₄₀), and zonulin were consistently decreased after caloric restriction.

Gut permeability was first measured using a mixture of four different sugars. Sucrose, used as a proxy for gastrointestinal permeability, significantly decreased after caloric restriction ($P = 0.012$). Two weeks after intervention, sucrose increased significantly again ($P = 0.006$). In contrast, mannitol, a marker for intestinal permeability, did not change significantly during the 28 days of caloric restriction ($P = 0.162$). However, after the post-intervention phase, its percental urine recovery was significantly increased ($P < 0.001$). Lactulose, used as a surrogate to monitor tight junction fitness significantly decreased during intervention ($P = 0.01$), while it relapsed afterwards ($P < 0.01$). Also, sucralose, used as colonic permeability marker, significantly decreased during VLCD ($P = 0.018$) and increased again after caloric restriction ($P = 0.019$).

In addition to sugar translocation, we used PEGs translocation as an additional measure of gut permeability. The mixture of the different molecular weights of PEG enabled size-dependent assessment of permeability properties of the mucosa. Translocation of PEG M_r 400 was significantly decreased after VLCD (Table 2). In the 2-week follow-up, these low molecular weight PEGs returned back to baseline levels. All larger homologues of different chain lengths (PEG₂₅, PEG₃₀, PEG₃₅, and PEG₄₀) significantly decreased after caloric restriction ($P < 0.01$ for each measurement), but remained stable during the subsequent two weeks. Similarly, PEG₇₀ and PEG₈₀ significantly decreased during the 28 days of caloric restriction and remained stable thereafter (Table 2).

Finally, zonulin was used as another marker of paracellular gut permeability²⁵. Plasma concentration at baseline declined significantly after the 4-week hypocaloric intervention ($P < 0.01$). After the subsequent two weeks, zonulin levels returned to baseline values ($P < 0.01$) (Table 2).

Effect of VLCD on adipokine expression and fat cell size. In the whole study population, gene expression in subcutaneous adipose tissue was assessed by qPCR and showed a significant down-regulation of leptin after VLCD in comparison to baseline ($P = 0.001$). In contrast, the expression of adiponectin, MCP-1, and cluster of differentiation 68 (CD68) were not significantly different before and after the hypocaloric intervention (Fig. 1)

From a subsample of participants, fat cell size from para-umbilical subcutaneous adipose tissue biopsies was measured before and after VLCD (Fig. 1). Adipocyte size before VLCD was $70.5 \pm 7.7 \mu\text{m}$ ($n = 8$) and decreased to $67.3 \pm 7.1 \mu\text{m}$ ($n = 8$) after caloric restriction without reaching significance ($P = 0.38$). Mean adipocyte surface area before VLCD was $4,478 \pm 997 \mu\text{m}^2$ and decreased to $4,020 \pm 773 \mu\text{m}^2$ ($n = 8$, $P = 0.31$).

Intervention triggered individual-specific changes in fecal microbiota profiles. After quality- and chimera-check, a total of 815,773 sequences clustering in 235 operational taxonomic units (OTU) were

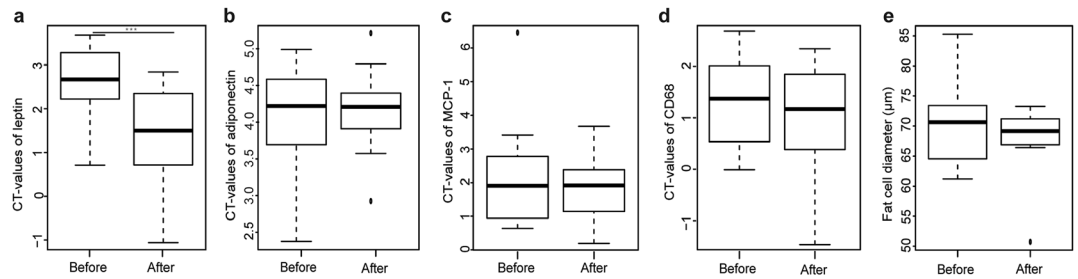


Figure 1. (a–d) Boxplots based on cycle threshold values (CT) of adipose tissue biopsies from 18 participants before and after the 4-week caloric restriction. (e) For fat cell diameters, data of 8 participants were available. *** $P < 0.001$.

analysed. Caloric restriction did not affect *alpha*-diversity (Fig. 2a). *Beta*-diversity analysis revealed marked inter-individual differences and no significantly distinct clustering according to time points (Fig. 1b). These data suggest that caloric restriction did not trigger consistent shifts in the overall phylogenetic makeup of fecal bacterial populations; microbiota profiles remained individual-specific throughout the study (Supplementary Fig. 2). The relative abundance of members of the phylum *Proteobacteria* was significantly decreased after caloric restriction. This decrease did not hold up after correction for multiple testing. No taxonomic groups within this phylum (e.g. *Enterobacteriaceae*) showed significant differences (Fig. 2c). Of the 235 OTUs detected, five showed significant differences in their relative abundances during intervention, as per explorative analysis (Fig. 2d). Three OTUs belonged to the family *Lachnospiraceae* within the phylum *Firmicutes*. OTU 8 (*Anaerostipes hadrus*, 100% sequence identity) and OTU 10 (*Blautia sp.*, several hits > 97% sequence identity) showed higher relative abundance after VLCD and returned to baseline values after two weeks. Relative abundances of OTU 1 (*Agathobacter rectalis*, 100% sequence identity) decreased after caloric restriction and throughout the end of the study. Two additional OTUs outside the *Lachnospiraceae* were characterised by intervention-related increase in their relative abundances: OTU 18 (*Ruminococcus faecis*, 100% sequence identity) within the *Ruminococcaceae* and OTU 3 (*Bifidobacterium sp.*, several hits > 97% sequence identity) within the family *Bifidobacteriaceae*.

Discussion

The purpose of our study was to assess the effect of a standardised 4-week caloric restriction on gut permeability, inflammatory markers, and fecal microbiota in obese women. As expected, the VLCD resulted in a significant decrease in body weight and fat mass as well as improvement of fasting blood glucose, insulin, HOMA-IR and lipid parameters.

The primary objective was to study whether gut permeability, which is reported to be impaired in obesity⁷, can be positively affected by caloric restriction. Our findings based on a variety of methods indicate that a standardised caloric restriction resulting in moderate weight loss significantly reduced gut permeability, in particular paracellular translocation. These data are consistent with results of a recent Chinese study reporting decreased gut permeability after a 9-week intervention diet consisting of traditional Chinese foods and prebiotics (1, 000–1,600 kcal/day)²⁶. However, our study extends this observation by providing a more comprehensive dataset using a variety of methods and a precisely defined diet. It is interesting to note that improved gut barrier function was observed along the gastrointestinal tract, as we measured clear response for sucrose reflecting gastroduodenal permeability down to sucralose, which is taken up in the colon. Likewise, decreases in the translocation of PEG particles of various sizes reflecting paracellular permeability were measured in urine samples. Zonulin, a physiological modulator of intercellular tight junctions²⁷, was also found to decrease during caloric restriction, but rapidly returned to baseline levels after restoring a normal diet. In conclusion, caloric restriction induced uniform and consistent changes towards decreased gut permeability.

To be able to distinguish between caloric restriction and weight loss, we studied the participants after returning to a balanced weight-maintaining diet for two consecutive weeks. The data suggest that most changes observed under the very low calorie diet disappeared, indicating that these changes were mainly due to the acute and marked caloric restriction rather than to the moderate decrease in body weight, as participants did not gain substantial weight during the two weeks of follow-up.

As expected, the plasma concentrations of the inflammation marker hsCRP were decreased after VLCD, which is in agreement with the literature²⁸. We also measured circulating LBP as a surrogate marker of translocation of cell wall components from Gram-negative bacteria, a term referred to as leaky gut-associated endotoxemia⁹. Caloric restriction induced a rather modest decrease in LBP levels²⁹, which is in line with the results of the gut permeability measurements and the possibly associated decrease in inflammatory markers. However, the design of the study does not allow to draw firm conclusions on the potential causal relationship between endotoxin translocation and systemic inflammation.

Plasma leptin levels decreased markedly, while HMW adiponectin increased after intervention. In contrast, levels of MCP-1 remained unchanged. One explanation could be that a mean weight loss of 7% is too small for a larger effect on obesity-related inflammation markers³⁰. In addition, the changes in gene expression for selected markers in adipose tissue – with the exception of leptin – were modest, probably due to the limited weight loss.

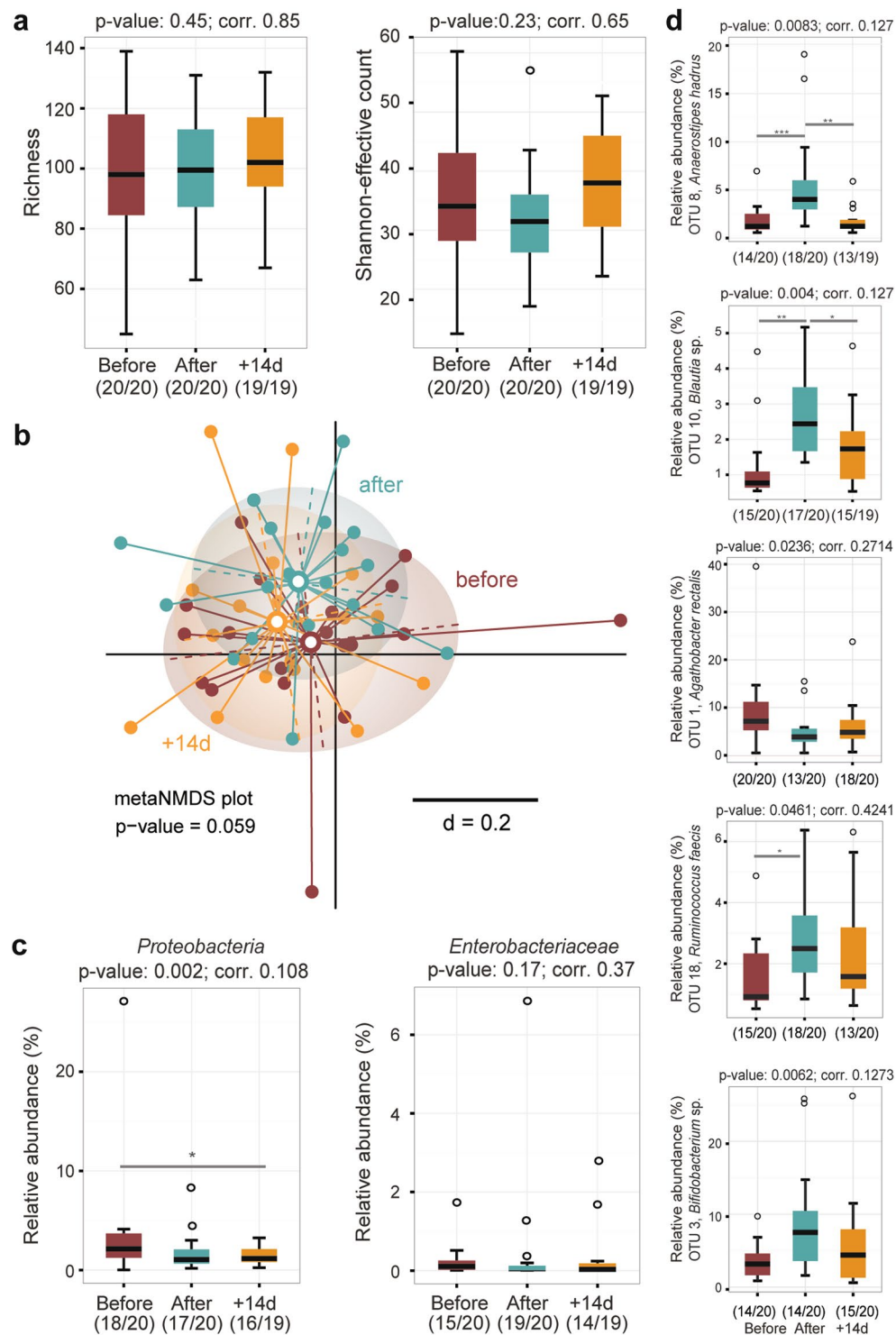


Figure 2. Fecal microbiota analysis by 16S rRNA gene amplicon analysis. **(a)** Diversity within samples (α -diversity) was estimated by species richness and Shannon-effective counts. **(b)** meta nonparametric multidimensional scaling plot of phylogenetic distances based on generalized UniFrac (β -diversity). **(c)** Occurrence of members of the phylum *Proteobacteria* and the family *Enterobacteriaceae*, including significance before and after Benjamini-Hochberg adjustment. **(d)** Relative abundances of five dominant OTUs showing significance overtime. *** $P < 0.001$; ** $P < 0.01$; * $P < 0.5$.

Despite the significant weight reduction, no significant decline in fat cell size of abdominal subcutaneous adipose tissue was observed. However, there a trend towards a decrease of the mean adipocyte size. Verhoef *et al.* showed that a 10% weight loss mediated a significant decline in adipocyte size³¹.

With respect to fecal microbiota profiles, the overall bacterial phylogenetic makeup was not substantially affected by caloric restriction in a consistent manner across all individuals. Moreover, we did not observe changes in *alpha*-diversity, in contrast to changes in richness reported in the context of host metabolic disturbances and nutritional intervention^{32,33}. Decreased relative abundances of *Proteobacteria* were observed, in agreement with other reports on their occurrence in individuals with impaired metabolic health^{34,35}. Relative abundances of the species *Anaerostipes hadrus* were increased by approximately two-fold after 28 days of caloric restriction and returned to baseline values after intervention. Although data in the present study are descriptive and exploratory, and no cause-effect relationship can be established, *A. hadrus* was described as a butyrate-producing bacterium^{36,37}, and butyrate is usually regarded as beneficial in the context of metabolic health^{38,39,32}. In contrast, median relative abundances of another butyrate-producing species, *Agathobacter rectalis*, were decreased from ca. 7 to 4% after caloric restriction. Additional studies including targeted metabolite measurements will be needed to clarify the impact of caloric restriction on butyrate production in the gut.

The intervention was also associated with an increased occurrence of one OTU in each the *Ruminococcus* and *Bifidobacterium* genus, which both include degraders of complex dietary and host-derived polysaccharides⁴⁰. Santacruz *et al.* also showed an increase in qPCR counts of *Bifidobacterium spp.* after weight loss (−6,9 kg) in obese adolescents following 10 weeks of caloric restriction⁴¹.

The strength of our study is the strict standardisation and the extensive phenotyping of the participants. In addition, an extensive array of different methods was used to characterise the impact of VLCD on gut permeability: The metabolic status was assessed by an oGTT; The inflammation status was investigated by a variety of circulating parameters as well as gene expression in adipose tissue samples. The results were further substantiated by data related to the gut microbiota, which followed an individual pattern. Additional studies are needed to better understand these heterogeneous responses.

In conclusion, our data suggest that a 4-week VLCD diet triggers beneficial effects on intestinal barrier function in obese women, which rapidly disappears after returning to a normal diet. The potential causal relationship between changes in gut permeability and the changes observed for metabolic and inflammatory biomarkers as well as specific target bacteria needs to be investigated in more detail.

Participants and Methods. The study protocol was reviewed and approved by the ethics committee of the Faculty of Medicine of the Technical University of Munich, Germany (approval no. 5499/12). The guidelines of the International Conference on Harmonization of Good Clinical Practice and the declaration of Helsinki (in the revised version of Seoul, South Korea 2008) was basis of the study. Written informed consent was obtained from all participants before inclusion into the study. The study was registered in the German Clinical Trial Register (DRKS00006210). The date of German Clinical Trial Register registration was 11th June 2014.

Study participants. Twenty female participants with a BMI ≥ 30 kg/m² were recruited in October 2013 via advertisements in the area of Munich, Germany. The participants' eligibility was assessed with a detailed screening questionnaire including their medical history. Exclusion criteria were: BMI < 30 kg/m², male, smoking, acute infections, severe diseases (e.g. cancer), treatment with oral anticoagulants or other antithrombotic medication, intestinal surgery in the last three months, autonomous neuropathy, or inflammatory intestinal diseases.

Intervention. Figure 3 summarises the study design of this single arm intervention trial. In total, the study duration was seven weeks and was structured into three time periods. During the first period, participants were instructed to maintain their usual eating habits. Then, participants underwent a caloric restriction using a defined formula diet of 800 kcal/day for 28 days. Finally, during the two weeks following intervention, participants were instructed to follow a balanced diet of 1,800 kcal/day. Before, immediately after, and two weeks after the formula diet intervention, clinical and biochemical parameters, gut permeability, and fecal microbiota profiles were assessed. Magnetic resonance imaging (MRI) of subcutaneous and visceral fat depots and a needle aspiration of periumbilical subcutaneous adipose tissue was carried out before and after the 4 weeks of hypocaloric intervention.

Diet protocols. The study participants were instructed to record their food consumption during the whole study period. The energy content and macronutrient composition of the diets were calculated using the OptiDiet Plus software (Version 5.1.2.046, GOE mbH, Linden, Germany).

Anthropometric measurements. Anthropometric and clinical measurements were performed in a standardised manner between 8 and 9 am in the morning following an overnight fast. Body weight and composition were measured using the TANITA Body Composition Analyzer Type BC-418 MA III (Amsterdam, Netherlands). The resting metabolic rate (RMR) was measured using a canopy hood (COSMED Quark RMR, Fridolfing, Germany).

Blood samples and biochemical analyses. Blood samples were collected in the fasting state. Lipid parameters (total cholesterol, LDL-c, HDL-c, triglycerides), liver enzymes (aspartate transaminase (AST), alanine transaminase (ALT), γ -glutamyltransferase (γ -GT)), creatinine, uric acid, and fasting glucose were analysed by SynLab (Munich, Germany). An additional blood sample was collected, immediately centrifuged (2, 500 g for 10 minutes at 20 °C) and subsequently stored at −80 °C until analysis. Leptin, chemerin, hsCRP, RANTES, MCP-1, HMW adiponectin, and LBP (all: R&D, Wiesbaden, Germany), insulin (Dako, Glostrup, Denmark), and zonulin (Immundiagnostik AG, Bensheim, Germany) were assayed in plasma using commercially available enzyme-linked immunosorbent assays (ELISA). Fecal calprotectin was measured by ELISA (CALPROLAB™ Calprotectin ELISA (HRP), FROST Diagnostika GmbH, Otterstadt, Germany). All ELISAs were performed as described by the manufacturers. NEFA were measured using a commercial test kit (Wako Chemicals GmbH,

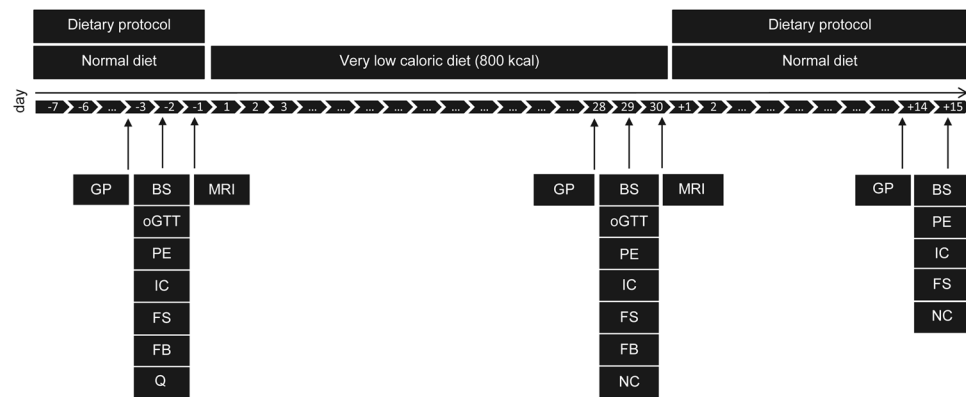


Figure 3. Study design. The scheme gives an overview of the timeline and different examinations performed. Abbreviations: BS, Blood sample; FB, fat biopsy; FS, fecal sample; GP, gut permeability; IC, indirect calorimetry; MRI, magnetic resonance imaging; NC, nutritional counseling; PE, physical examination; oGTT, oral glucose tolerance test; Q, questionnaire.

Neuss, Germany). Insulin resistance was estimated using the HOMA-IR, $[\text{HOMA-IR} = \text{insulin } (\mu\text{U/mL}) \times \text{glucose (mmol/L)} / 22.5]$ ⁴².

Oral glucose tolerance test. Oral glucose tolerance tests (OGTT) began between 8 am and 9 am following a 12-hour overnight fast. After taking a baseline blood sample, volunteers received 75 g glucose in a volume of 300 ml (AccuCheck®-O.G.T., Roche, Mannheim, Germany). After 30, 60 and 120 minutes blood was drawn and glucose levels were determined (HemoCue Glucose 201⁺, plasma-calibrated, Ängelholm, Sweden).

Gut permeability. Gut barrier function was assessed by means of different non-invasive tests. First, the intestinal permeability was measured via a validated sugar absorption test and a test using PEG. Both tests were performed in parallel. The principle is to measure urine excretion of orally administered substances of different molecular masses. The tests were done directly before intervention, after intervention, and two weeks after intervention. Data are presented as percentage of ingested sugars and PEGs that were discovered in the urine, referred to as % urine recovery. Finally, the gut permeability marker zonulin was measured in blood via ELISA.

Sugar absorption test. The sugar absorption test was performed as described by Norman *et al.*⁴³. The sugars were quantified by high-performance liquid chromatography with pulsed electrochemical detection (chromatography module: 250, Dionex, Idstein, Germany)⁴³.

Polyethylene glycol absorption test. Participants received 100 ml of a PEG test solution containing 1 mg of molecular mass (M_r) 400 (PEG₆-PEG₁₃; mass range: 285–678 Da), 200 mg of M_r 1500 (PEG₂₀-PEG₄₅; mass range: 899–2,000 Da), 4 g of M_r 3000 (PEG₅₁-PEG₉₀; mass range: 2,264–3,982 Da), and 4 g of M_r 4000 (PEG₇₅-PEG₁₁₅; mass range: 3,322–5,084 Da) (Merck Darmstadt, Germany). Five hours after ingestion of the sugar test solution, the PEG test solution was drunk and urine was sampled during the following 24 hours. PEGs were analysed by liquid chromatography-mass spectrometry as described by Lichtenegger and Rychlik⁴⁴.

Abdominal subcutaneous adipose tissue biopsy. Abdominal subcutaneous adipose tissue specimens were obtained by needle aspiration before and after the formula diet. After washing in Krebs-Ringer-buffer, fat tissue was aliquoted into tubes containing sterilised zirconia-glas-beads (Carl Roth, Karlsruhe, Germany), RLT-buffer (RNeasy Mini Kit, Qiagen, Hilden, Germany) and 1% (v/v) β -mercaptoethanol (#M3148, Sigma-Aldrich, St. Louis, Missouri, USA), and then immediately frozen and stored at -80°C . For fat histology, fat tissue was fixed in 4% buffered formalin (pH 7.4) for 24 h and finally embedded in paraffin and stored at room temperature until analysis. Determination of adipocyte size was done by using the open source cellprofiler® image analysis software (<http://www.cellprofiler.org/>).

Quantitative polymerase chain reaction. The expression of specific target genes was assessed by using quantitative polymerase chain reaction (qPCR). The primer sequences used are shown in Supplemental Table 1. qPCR was performed using the Mastercycler® ep realplex (Eppendorf, Hamburg, Germany). Target and house-keeping gene amplicons were detected using SYBR Green (Thermo Fisher, Scientific, Darmstadt, Germany). Importin 8 (IPO8) and peptidylprolyl isomerase A (PPIA) were used for normalization^{45,46}. Each sample was run in duplicate, and negative controls without cDNA were included. The calculation of relative expression was performed by using the relative expression software tool REST© (<http://rest.gene-quantification.info/>)⁴⁷.

Fecal samples. Fecal samples were collected directly into sterile plastic containers (1,000 ml; VWR International, Munich, Germany). Participants were then asked to collect one plastic spoon at one location of the fecal material into a stool collection tube containing 8 ml DNA stabilization buffer (Stratec Molecular GmbH, Berlin, Germany). Afterwards, fecal samples were immediately frozen at -18°C until the next visit. Participants

transported the frozen fecal samples by using cooling aggregates to the lab. Finally, collection tubes were immediately stored at -80°C .

High-throughput 16S ribosomal RNA gene amplicon sequencing. Samples were processed as described previously⁴⁸. Briefly, cells were lysed by bead-beating and heat-treatment and the metagenomic DNA was purified using gDNA columns (Macherey-Nagel, Düren, Germany). Concentrations and purity were inspected using the NanoDrop[®] system (Thermo Scientific Waltham, Massachusetts, USA). The V3/V4 region of 16S ribosomal RNA (rRNA) genes was amplified (25 cycles) from 24 ng DNA using primers 341 F and 785 R⁴⁹. After purification (AMPure XP system, Beckmann Coulter Biomedical GmbH) and pooling in an equimolar amount, the 16S rRNA gene amplicons were sequenced in paired-end modus (PE275) using a MiSeq system (Illumina, Inc., San Diego, California, USA) following the manufacturer's instructions and a final DNA concentration of 10 pM and 15% (v/v) PhiX standard library.

Sequence analysis. Raw read files were processed based on the UPARSE approach⁵⁰ using IMNGS⁵¹. Sequences were tested for the presence of chimeras using UCHIME⁵² and OTUs were clustered at a threshold of 97% sequence similarity. To avoid analysis of spurious OTUs, only those with a relative abundance $> 0.5\%$ total sequences in at least one sample were kept. SILVA (SILVA Incremental Aligner version 1.2.11)⁵³ and RDP classifier (set 15; 80% confidence)⁵⁴ were used to assign taxonomic classification to the OTUs representative sequences. Specific OTUs with differential abundances between groups were further identified using EzTaxon. Phylogenetic relationships were examined using the generalized UniFrac procedure⁵⁵. Shannon-effectiveness counts were determined to estimate diversity within samples (*alpha*-diversity) as described by Jost *et al.*⁵⁶.

Statistical analyses. Data were analysed in the R programming environment. Anthropometric and metabolic data are presented as mean \pm standard deviation. *P*-values < 0.05 were regarded as statistically significant. According to data distribution, paired Student's test was applied to assess mean differences before and after the formula diet. Rhea (v1.0.1-5) was used for analysis of fecal microbiota profiles⁵⁷. The effect of VLCD on OTUs and taxonomic counts was tested using Friedman Rank Test for the analysis of a nonparametric randomized block design. Missing values were handled by using Skillings-Mack test. Wilcoxon Signed Rank Sum Test for matched pairs was applied for pairwise comparisons. The Benjamini-Hochberg method was used for adjustment after multiple testing. For *beta*-diversity analysis, generalized UniFrac distances were calculated using the package GUniFrac⁵⁵.

References

- Kahn, S. E., Hull, R. L. & Utzschneider, K. M. Mechanisms linking obesity to insulin resistance and type 2 diabetes. *Nature* **444**, 840–846 (2006).
- Shoelson, S. E., Lee, J. & Goldfine, A. B. Inflammation and insulin resistance. *The Journal of clinical investigation* **116**, 1793–1801 (2006).
- Hansson, G. K. Inflammation, atherosclerosis, and coronary artery disease. *The New England journal of medicine* **352**, 1685–1695 (2005).
- Weisberg, S. P. *et al.* Obesity is associated with macrophage accumulation in adipose tissue. *The Journal of clinical investigation* **112**, 1796–1808 (2003).
- Xu, H. *et al.* Chronic inflammation in fat plays a crucial role in the development of obesity-related insulin resistance. *The Journal of clinical investigation* **112**, 1821–1830 (2003).
- Skurk, T. & Alberti-Huber, C. Herder, C. & Hauner, H. Relationship between adipocyte size and adipokine expression and secretion. *The Journal of clinical endocrinology and metabolism* **92**, 1023–1033 (2007).
- Teixeira, T. *et al.* Intestinal permeability parameters in obese patients are correlated with metabolic syndrome risk factors. *Clinical nutrition (Edinburgh, Scotland)* **31**, 735–740 (2012).
- Creely, S. J. *et al.* Lipopolysaccharide activates an innate immune system response in human adipose tissue in obesity and type 2 diabetes. *American journal of physiology. Endocrinology and metabolism* **292**, E740–7 (2007).
- Cani, P. D. *et al.* Changes in gut microbiota control metabolic endotoxemia-induced inflammation in high-fat diet-induced obesity and diabetes in mice. *Diabetes* **57**, 1470–1481 (2008).
- Falony, G. *et al.* Population-level analysis of gut microbiome variation. *Science (New York, N.Y.)* **352**, 560–564 (2016).
- Ley, R. E., Turnbaugh, P. J., Klein, S. & Gordon, J. I. Microbial ecology: human gut microbes associated with obesity. *Nature* **444**, 1022–1023 (2006).
- Zhang, H. *et al.* Human gut microbiota in obesity and after gastric bypass. *Proceedings of the National Academy of Sciences of the United States of America* **106**, 2365–2370 (2009).
- Schwartz, A. *et al.* Microbiota and SCFA in lean and overweight healthy subjects. *Obesity (Silver Spring, Md.)* **18**, 190–195 (2010).
- Cani, P. D. *et al.* Changes in gut microbiota control inflammation in obese mice through a mechanism involving GLP-2-driven improvement of gut permeability. *Gut* **58**, 1091–1103 (2009).
- de La Serre, C. B. *et al.* Propensity to high-fat diet-induced obesity in rats is associated with changes in the gut microbiota and gut inflammation. *American journal of physiology. Gastrointestinal and liver physiology* **299**, G440–8 (2010).
- Moreno-Navarrete, J. M. *et al.* Circulating lipopolysaccharide-binding protein (LBP) as a marker of obesity-related insulin resistance. *International journal of obesity (2005)* **36**, 1442–1449 (2012).
- Cobden, I., Rothwell, J. & Axon, A. T. Intestinal permeability and screening tests for coeliac disease. *Gut* **21**, 512–518 (1980).
- Bjarnason, I., Peters, T. J. & Veall, N. A persistent defect in intestinal permeability in coeliac disease demonstrated by a ⁵¹Cr-labelled EDTA absorption test. *Lancet (London, England)* **1**, 323–325 (1983).
- Morales, M. T., Montaña, M. T., Galan, G. & Gomez Ariza, J. L. Spectrophotometric determination of bismuth in pharmaceutical preparations using 1-[di(2-pyridyl)-methylene]-5-salicylidene-thiocarbonohydrazide. *Farmaco (Società chimica italiana: 1989)* **45**, 673–682 (1990).
- Troncone, R., Caputo, N., Florio, G. & Finelli, E. Increased intestinal sugar permeability after challenge in children with cow's milk allergy or intolerance. *Allergy* **49**, 142–146 (1994).
- Cottam, D. R. *et al.* The chronic inflammatory hypothesis for the morbidity associated with morbid obesity: implications and effects of weight loss. *Obesity surgery* **14**, 589–600 (2004).

22. Clément, K. *et al.* Weight loss regulates inflammation-related genes in white adipose tissue of obese subjects. *FASEB journal: official publication of the Federation of American Societies for Experimental Biology* **18**, 1657–1669 (2004).
23. Lehrke, M. *et al.* Chemerin is associated with markers of inflammation and components of the metabolic syndrome but does not predict coronary atherosclerosis. *European journal of endocrinology* **161**, 339–344 (2009).
24. Bozaoglu, K. *et al.* Chemerin is a novel adipokine associated with obesity and metabolic syndrome. *Endocrinology* **148**, 4687–4694 (2007).
25. Fasano, A. *et al.* Zonulin, a newly discovered modulator of intestinal permeability, and its expression in coeliac disease. *Lancet (London, England)* **355**, 1518–1519 (2000).
26. Xiao, S. *et al.* A gut microbiota-targeted dietary intervention for amelioration of chronic inflammation underlying metabolic syndrome. *FEMS Microbiol Ecol* **87**, 357–367 (2014).
27. Fasano, A. Regulation of intercellular tight junctions by zonula occludens toxin and its eukaryotic analogue zonulin. *Annals of the New York Academy of Sciences* **915**, 214–222 (2000).
28. Bassuk, S. S., Rifai, N. & Ridker, P. M. High-sensitivity C-reactive protein: clinical importance. *Current problems in cardiology* **29**, 439–493 (2004).
29. Zhang, C. *et al.* Structural modulation of gut microbiota in life-long calorie-restricted mice. *Nature communications* **4**, 2163 (2013).
30. Forsythe, L. K. W., Julie, M. W. & Livingstone, M. Barbara E. Obesity and inflammation: the effects of weight loss. *Nutrition research reviews* **21**, 117–133 (2008).
31. Verhoef, S. P. M. *et al.* Physiological response of adipocytes to weight loss and maintenance. *PLoS ONE* **8**, e58011 (2013).
32. Le Chatelier, E. *et al.* Richness of human gut microbiome correlates with metabolic markers. *Nature* **500**, 541–546 (2013).
33. Cotillard, A. *et al.* Dietary intervention impact on gut microbial gene richness. *Nature* **500**, 585–588 (2013).
34. Shin, N.-R., Whon, T. W. & Bae, J.-W. Proteobacteria: microbial signature of dysbiosis in gut microbiota. *Trends in biotechnology* **33**, 496–503 (2015).
35. Xiao, S. *et al.* A gut microbiota-targeted dietary intervention for amelioration of chronic inflammation underlying metabolic syndrome. *FEMS microbiology ecology* **87**, 357–367 (2014).
36. Allen-Vercoe, E. *et al.* *Anaerostipes hadrus* comb. nov. a dominant species within the human colonic microbiota; reclassification of *Eubacterium hadrum* Moore *et al.* 1976. *Anaerobe* **18**, 523–529 (2012).
37. Kant, R., Rasinkangas, P., Satokari, R., Pietila, T. E. & Palva, A. Genome Sequence of the Butyrate-Producing Anaerobic Bacterium *Anaerostipes hadrus* PEL 85. *Genome Announcements* **3** (2015).
38. Vrieze, A. *et al.* Transfer of intestinal microbiota from lean donors increases insulin sensitivity in individuals with metabolic syndrome. *Gastroenterology* **143**, 913–6.e7 (2012).
39. Derrien, M. & Veiga, P. Rethinking Diet to Aid Human-Microbe Symbiosis. *Trends in microbiology* **25**, 100–112 (2017).
40. Baer, D. J. *et al.* The metabolizable energy of dietary resistant maltodextrin is variable and alters fecal microbiota composition in adult men. *The Journal of nutrition* **144**, 1023–1029 (2014).
41. Santacruz, A. *et al.* Interplay between weight loss and gut microbiota composition in overweight adolescents. *Obesity (Silver Spring, Md.)* **17**, 1906–1915 (2009).
42. Matthews, D. R. *et al.* Homeostasis model assessment: insulin resistance and beta-cell function from fasting plasma glucose and insulin concentrations in man. *Diabetologia* **28**, 412–419 (1985).
43. Norman, K. *et al.* Increased intestinal permeability in malnourished patients with liver cirrhosis. *European journal of clinical nutrition* **66**, 1116–1119 (2012).
44. Lichtenegger, M. & Rychlik, M. Development of a stable isotope dilution LC-MS assay for the quantitation of multiple polyethylene glycol (PEG) homologues to be used in permeability studies. *Journal of chromatography. B, Analytical technologies in the biomedical and life sciences* **1001**, 182–190 (2015).
45. Dankel, S. N. *et al.* COL6A3 expression in adipocytes associates with insulin resistance and depends on PPARgamma and adipocyte size. *Obesity (Silver Spring, Md.)* **22**, 1807–1813 (2014).
46. McCulloch, L. J. *et al.* COL6A3 is regulated by leptin in human adipose tissue and reduced in obesity. *Endocrinology* **156**, 134–146 (2015).
47. Pfaffl, M. W., Horgan, G. W. & Dempfle, L. Relative expression software tool (REST) for group-wise comparison and statistical analysis of relative expression results in real-time PCR. *Nucleic acids research* **30**, e36 (2002).
48. Lagkouvardos, I. *et al.* Gut metabolites and bacterial community networks during a pilot intervention study with flaxseeds in healthy adult men. *Molecular nutrition & food research* **59**, 1614–1628 (2015).
49. Klindworth, A. *et al.* Evaluation of general 16S ribosomal RNA gene PCR primers for classical and next-generation sequencing-based diversity studies. *Nucleic acids research* **41**, e1 (2013).
50. Edgar, R. C. UPARSE: highly accurate OTU sequences from microbial amplicon reads. *Nature methods* **10**, 996–998 (2013).
51. Lagkouvardos, I. *et al.* IMNGS: A comprehensive open resource of processed 16S rRNA microbial profiles for ecology and diversity studies. *Scientific reports* **6**, 33721 (2016).
52. Edgar, R. C. Search and clustering orders of magnitude faster than BLAST. *Bioinformatics (Oxford, England)* **26**, 2460–2461 (2010).
53. Quast, C. *et al.* The SILVA ribosomal RNA gene database project: improved data processing and web-based tools. *Nucleic acids research* **41**, D590–6 (2013).
54. Wang, Q., Garrity, G. M., Tiedje, J. M. & Cole, J. R. Naive Bayesian classifier for rapid assignment of rRNA sequences into the new bacterial taxonomy. *Applied and Environmental Microbiology* **73**, 5261–5267 (2007).
55. Chen, J. *et al.* Associating microbiome composition with environmental covariates using generalized UniFrac distances. *Bioinformatics (Oxford, England)* **28**, 2106–2113 (2012).
56. Jost, L. Partitioning diversity into independent alpha and beta components. *Ecology* **88**, 2427–2439 (2007).
57. Lagkouvardos, I., Fischer, S., Kumar, N. & Clavel, T. Rhea: a transparent and modular R pipeline for microbial profiling based on 16S rRNA gene amplicons. *PeerJ* **5**, e2836 (2017).

Acknowledgements

We are grateful to Dr. Claudia Eichhorn for performing needle aspiration, Julius Honecker for excellent support in measuring fat cell size, Dr. Karin Norman for her support regarding measurement of gut permeability, Manuela Hubersberger for her excellent technical assistance, and Caroline Ziegler as well as Angela Sachsenhauser of the ZIEL Core Facility Microbiome/NGS for their outstanding support with sample processing for high-throughput sequencing. This study was funded by the BMBF (Federal Ministry of Education and Research, grant no. 0315674). The formula diet was kindly provided by Nutrition Santé SAS (Revel, France).

Author Contributions

The authors' responsibilities were as follows – H.H., T.S., and B.O.: designed the research and study design; B.O.: was responsible for the data collection and trial management; L.H.: performed needle aspiration; D.H. and M.R.: provided essential reagents and materials; J.B.: was responsible for the sugar absorption test; T.K.:

analysed the PEGs; B.O.: performed ELISAs and the analysis of dietary records; B.O., I.L., T.C., S.F.: performed microbiota analysis and statistical analysis; B.O., T.C., T.S., and H.H.: wrote the manuscript; and all authors read and approved the final manuscript.

Additional Information

Supplementary information accompanies this paper at <https://doi.org/10.1038/s41598-017-12109-9>.

Competing Interests: The authors declare that they have no competing interests.

Publisher's note: Springer Nature remains neutral with regard to jurisdictional claims in published maps and institutional affiliations.



Open Access This article is licensed under a Creative Commons Attribution 4.0 International License, which permits use, sharing, adaptation, distribution and reproduction in any medium or format, as long as you give appropriate credit to the original author(s) and the source, provide a link to the Creative Commons license, and indicate if changes were made. The images or other third party material in this article are included in the article's Creative Commons license, unless indicated otherwise in a credit line to the material. If material is not included in the article's Creative Commons license and your intended use is not permitted by statutory regulation or exceeds the permitted use, you will need to obtain permission directly from the copyright holder. To view a copy of this license, visit <http://creativecommons.org/licenses/by/4.0/>.

© The Author(s) 2017